International Journal of Heat and Mass Transfer 235 (2024) 126182

Contents lists available at ScienceDirect

International Journal of Heat and Mass Transfer

journal homepage: www.elsevier.com/locate/ijhmt

Periodicity alters topological states in thermal diffusion system

Zhaochen Wang [a], Tianfeng Liu [a], Zhan Zhu [a], Xiaobing Luo [a], Run Hu [a,b,*]

[a] School of Energy and Power Engineering, Huazhong University of Science and Technology, Wuhan 430074, PR China
[b] Department of Applied Physics, Kyung Hee University, Yongin-Si, Gyeonggi-do 17104, Republic of Korea

ARTICLE INFO

Keywords:
Thermal diffusion
Thermal metamaterials
Topological states
Boundary conditions

ABSTRACT

Topological edge states are a ubiquitous phenomenon across diverse wave systems, including electromagnetic, acoustic and quantum systems. In contrast to wave systems, thermal transport is a kind of diffusion system characterized by pure dissipation. The imposition of different boundary conditions can significantly influence the evolution of thermal system, leading to the appearance of different topological states, which haven't been systematically analyzed yet, especially in practical heat transfer structures. In this work, via a non-Hermitian thermal diffusion lattice model, we discuss the periodicity-dependent topological states. Through rigorous theoretical analysis and numerical simulations of the temperature field, the Hamiltonian is obtained whose eigenvalues are purely imaginary corresponding to the decay rate of the temperature field. Our work paves the way for the investigation of how periodicity alters topological states in thermal diffusion systems, potentially revolutionizing the design of thermal metamaterials for topological thermal protection in thermal management.

1. Introduction

The recent years have witnessed a booming research of topological states in condensed matter physics, such as topological insulator [1,2], quantum Hall effect [3], twistronics [4], etc. Due to the similarity between wave equations and Schrödinger equations [5,6], the concept of topological states has also been extended to classical wave systems, including electromagnetic [7], photonics [8–10], acoustics [11]. More intriguing topological states have been revealed, such as high-order topological states [12,13] and Chern insulators [14,15]. The allure of such kind of research has grown exponentially in recent years for their promising applications in advanced magnetoelectronic and optoelectronic devices, which hold the potential to revolutionize the technological landscapes [16].

Recently, the exploration of topological phenomena in diffusion systems has garnered increasing attention, particularly in the field of heat transfer [17–20]. Heat conduction is naturally a purely dissipative process, and can be regulated by thermal metamaterials [21–25], which have been engineered to exhibit many novel thermal functionalities, such as thermal cloaking [26,27], concentrating [28,29], printing [30], camouflaging [31], etc. Moreover, thermal metamaterials also offer an excellent platform for the study of non-Hermitian physics [32–35]. For instance, integrating topological concepts into thermal management can achieve robust heat regulation against defects and disorder based on the Su-Schrieffer-Heeger (SSH) model [36–38] and non-Hermitian skin effects [39–41]. Recently, experimental observations of diffusion topological edge states have been reported in one-dimensional and two-dimensional SSH thermal lattice [42,43]. Nonetheless, as we know the boundary conditions (BCs) play the dominant role on heat conduction, the pronounced influence of BCs on topological states in thermal diffusion system haven't been systematically discussed yet. In particular, the periodicity of BCs can even break or change the topological states of the system, which calls for comprehensive discussion to clarify the periodicity-dependent topological states in thermal diffusion system.

In this work, similar to the SSH lattices we developed a two-dimensional topological thermal transport model. Through rigorous theoretical analysis and numerical simulations of the temperature field, we obtain the Hamiltonian of system and elucidate how periodicity alters various topological states in thermal diffusion system. Our study could pave the way for the development of novel thermal metamaterials with potential application for topological thermal protection, efficient thermal management, and directional heat transfer.

2. Topological thermal transport model

In order to migrate topological states from wave system to diffusion system, we develop a two-dimensional topological thermal transport

* Corresponding author.
E-mail address: hurun@hust.edu.cn (R. Hu).

https://doi.org/10.1016/j.ijheatmasstransfer.2024.126182
Received 4 July 2024; Received in revised form 29 August 2024; Accepted 6 September 2024

model by drawing inspiration from the thermal analogue of SSH lattices. In this model, topological thermal unit cells are arranged along the x and y directions to construct the thermal lattice. As depicted in Fig. 1(a), each topological thermal unit cell consists of four thermal sites, considered as thermal analogs of atoms in atomic lattices. Intercellularly and intracellularly, these thermal sites are connected through a network of different thermal channels with different thermal diffusion coefficients $D_{1,2}$. The whole model has unified heat capacity c_p, density ρ, and thermal conductivity κ. And each site has an identical radius R_0 and height h. The distance between each site is held constant at a_0, ensuring the lengths of the intra-coupling and inter-coupling thermal channels are equivalent. These channels are distinguished by their radius R_1 and R_2, which correspond to the thermal diffusion coefficients D_1 and D_2 respectively.

Our model allows for the facile manipulation of the intra-coupling and inter-coupling diffusion coefficients by adjusting the R_1 and R_2, as

$$D_{1,2} = \frac{\kappa}{\rho c_p} \cdot \frac{R_{1,2}^2}{R_0^2 a_0 h}. \tag{1}$$

By discretizing the heat conduction equation $\rho c \frac{\partial T}{\partial t} = \nabla q$, the evolution of the temperature field in this model can be described as

$$\begin{aligned} \frac{\partial T_{i,j}}{\partial t} &= D_{i-1,j}\left[T_{i-1,j} - T_{i,j}\right] + D_{i+1,j}\left[T_{i+1,j} - T_{i,j}\right] \\ &+ D_{i,j-1}\left[T_{i,j-1} - T_{i,j}\right] + D_{i,j+1}\left[T_{i,j+1} - T_{i,j}\right] \end{aligned} \tag{2}$$

where subscripts i, j denote the sequence indices of the thermal sites along the x and y direction respectively.$D_{a,b} = k/\rho$crepresents the thermal diffusion coefficient of thermal channels between thermal site i, j and thermal site a, b ($a = i-1, i, i+1$; $b = j-1, j, j+1$). $T_{i,j}$ represents the temperature of the thermal site i, j. By manually adjusting the radius, we can arbitrarily control the intra-coupling and inter-coupling diffusion coefficients with a certain ratio $\delta = D_2/D_1$.

We delineate a thermal unit cell by designating its four thermal sites as A, B, C, and D. Thus the temperature field in this thermal unit cell can be described as

$$\begin{cases} \frac{\partial T_{m,n,A}}{\partial \tau} = -D_1\left[2(1+\delta)\cdot T_{m,n,A} - \delta\cdot T_{m-1,n,B} - \delta\cdot T_{m,n+1,C} - T_{m,n,C} - T_{m,n,B}\right] \\ \frac{\partial T_{m,n,B}}{\partial \tau} = -D_1\left[2(1+\delta)\cdot T_{m,n,B} - \delta\cdot T_{m,n+1,D} - \delta\cdot T_{m+1,n,A} - T_{m,n,A} - T_{m,n,D}\right] \\ \frac{\partial T_{m,n,C}}{\partial \tau} = -D_1\left[2(1+\delta)\cdot T_{m,n,C} - \delta\cdot T_{m-1,n,D} - \delta\cdot T_{m-1,n,A} - T_{m,n,A} - T_{m,n,D}\right] \\ \frac{\partial T_{m,n,D}}{\partial \tau} = -D_1\left[2(1+\delta)\cdot T_{m,n,D} - \delta\cdot T_{m,n-1,B} - \delta\cdot T_{m+1,n,C} - T_{m,n,C} - T_{m,n,B}\right] \end{cases} \tag{3}$$

where subscripts m, n denote the sequence indices of unit cells along the x and y direction respectively. The governing equation of the thermal field can be articulated as:

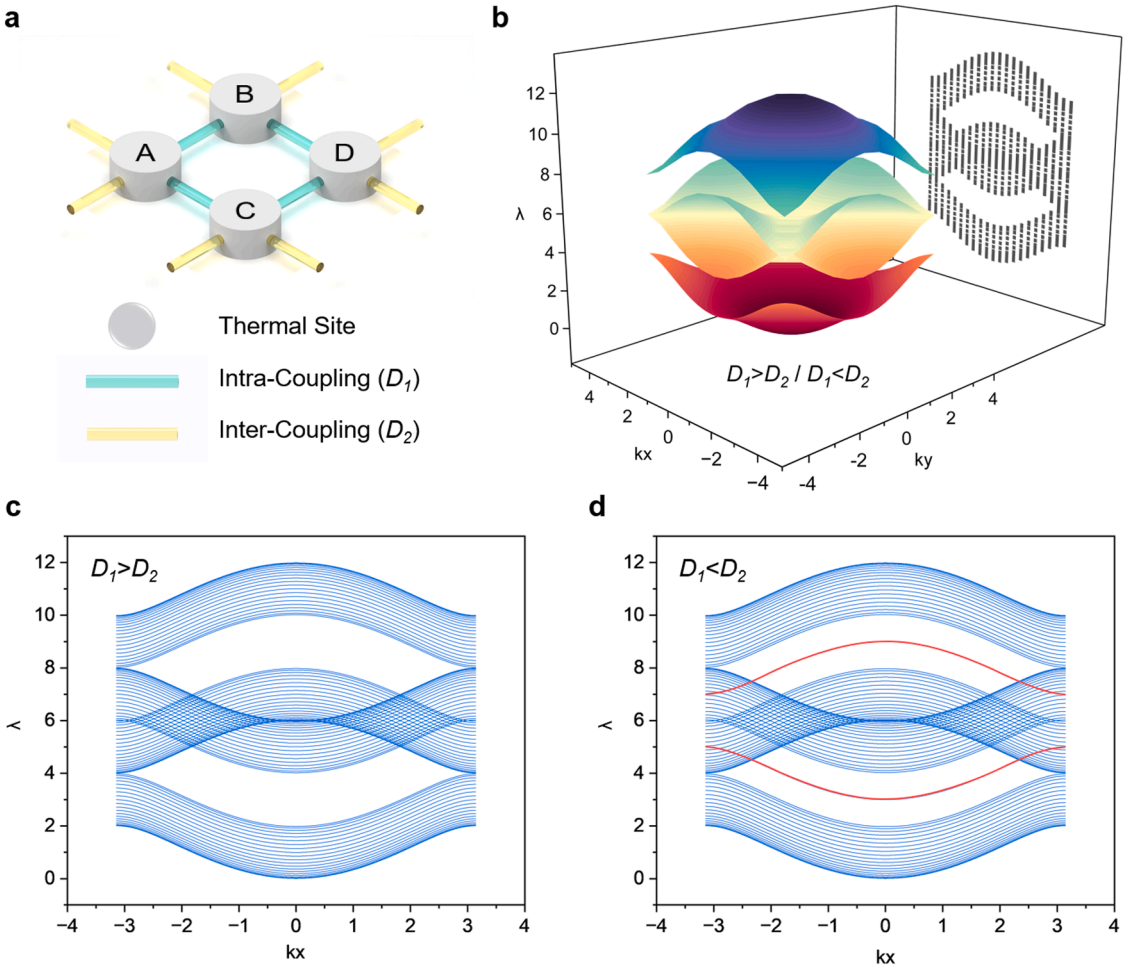

Fig. 1. (a) Schematic diagram of a topological thermal unit cell. (b) Eigen spectrum of periodic thermal lattice systems and the projection of eigen spectrum on the $k_x - \lambda$ plane. (c, d) Eigen spectrums under the trivial state and untrivial state when the system is periodic in one direction and fixed in the other direction. (The red curves represent the corresponding edge states).

$$\frac{\partial \widehat{T}}{\partial t} = -iH\widehat{T} \tag{4}$$

where $T = [\,T_{1,1,A} \quad T_{1,1,B} \quad \cdots \quad T_{m,n,D}\,]^T$, and H is the governing Hamiltonian. In contrast to wave systems, the Hamiltonian of the thermal transport model is characterized by a purely imaginary eigen spectrum ω for the purely dissipative nature of heat conduction. The imaginary eigenvalue corresponds to the thermal diffusion rate λ of the thermal transport model ($\lambda = -\mathrm{Im}(\omega)$).

Then we apply the periodic BCs, the Bloch Hamiltonian of this topological thermal transport model can be written as:

$$H(\mathrm{k}) = -i{\cdot}D_1{\cdot}\begin{bmatrix} 2(1+\delta) & -1-\delta e^{-ikx} & 0 & -1-\delta e^{-iky} \\ -1-\delta e^{ikx} & 2(1+\delta) & -1-\delta e^{-iky} & 0 \\ 0 & -1-\delta e^{iky} & 2(1+\delta) & -1-\delta e^{ikx} \\ -1-\delta e^{iky} & 0 & -1-\delta e^{-ikx} & 2(1+\delta) \end{bmatrix} \tag{5}$$

The eigen spectrum of the thermal transport model under periodic BCs is depicted in Fig. 1(b). It can be observed that the eigen spectrum consists of four energy bands, interspersed with two open bandgaps. In addition, we demonstrate the projection of the eigen spectrum on the k_x $-\lambda$ plane to better observe the distribution of eigenvalues. It should be noted that under such periodic BCs, regardless of $\delta < 1$ or $\delta > 1$, the fundamental characteristics of the eigenvalue distribution do not change, exhibiting a similar spectrum. To observe edge states in our model, we impose fixed BCs in one direction and maintain periodic BCs in the other. Then, by adjusting the ratio of the diffusion coefficients δ, we observe a variety of outcomes as illustrated in Fig. 1(c, d). When $\delta < 1$, the inter-coupling diffusion coefficient (D_2) is less than the intra-coupling diffusion coefficient (D_1), and the eigen spectrum exhibits two bandgaps, akin to the projection of the eigen spectrum under periodic BCs. Now the system is characterized by a topological trivial state. Conversely, when $\delta > 1$, the inter-coupling diffusion coefficient (D_2) exceeds the intra-coupling diffusion coefficient (D_1). Now unique bands appear in each of the two band gaps, which are marked by red. This appearance signifies the presence of edge states, and now the system is under a topological untrivial state.

3. Thermal topological states in practical thermal diffusion models

Our research has revealed that breaking the periodicity of the topological thermal transport model in a single direction will contribute the appearance of edge states. So what if the BCs are fixed in both directions? It is worth highlighting that in the practical heat transfer models, achieving structures with periodic BCs is often challenging. Typically, the application of periodic ordering metamaterials necessitates the use of an equivalent finite array structure. While examining

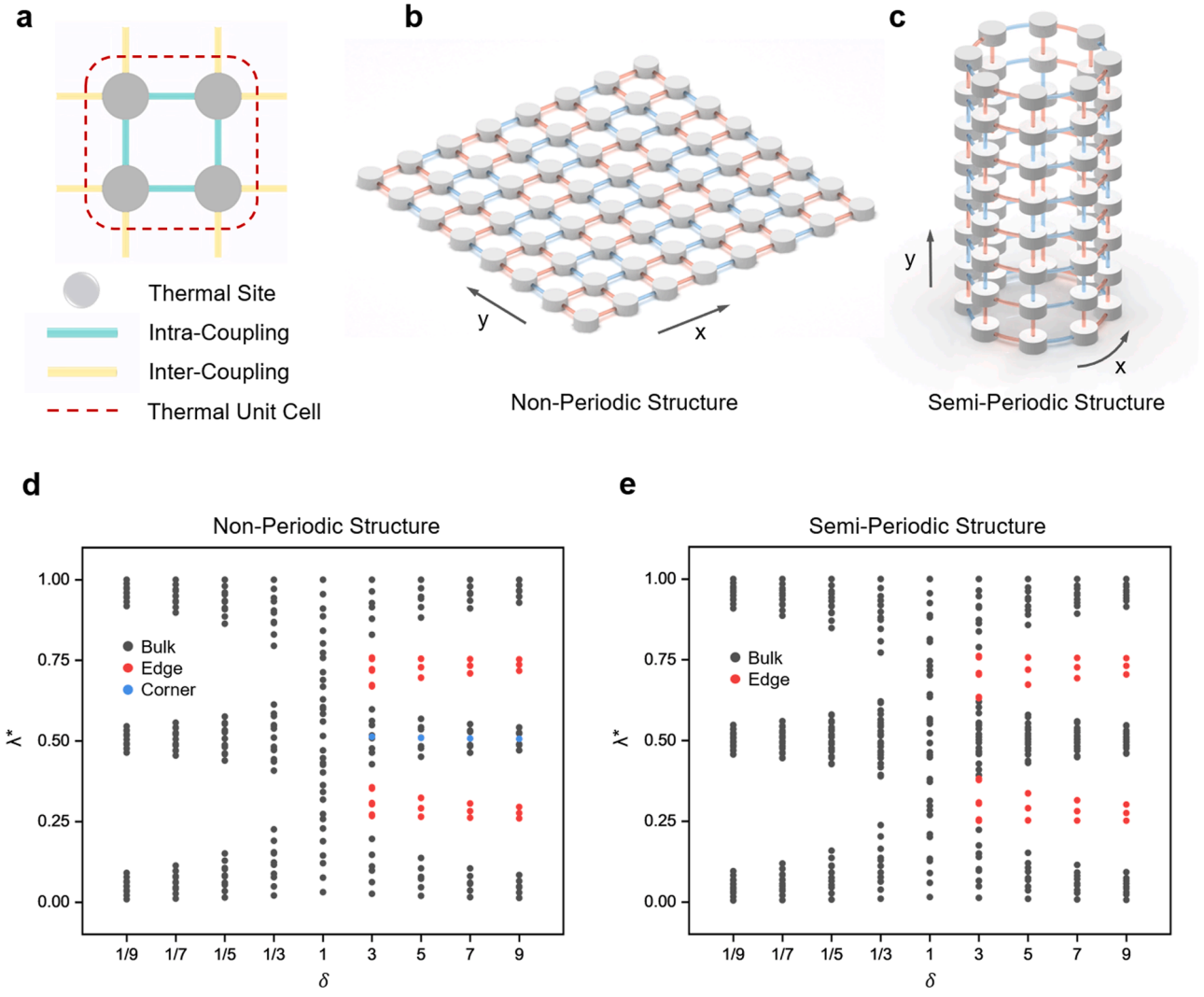

Fig. 2. (a) Schematic diagram of a topological thermal unit cell. (b, c) Schematic diagram of a non-periodic thermal diffusion lattice structure and a semi-periodic thermal diffusion lattice structure. (d, e) Eigen spectrum of non-periodic and semi-periodic thermal diffusion lattice structure.

topological phenomena under fixed BCs model aligns more closely with real-world heat conduction process and holds greater potential for applications.

We develop two kinds of tangible thermal meta structures to further investigate the effect of periodic boundaries on topological phenomena in practical thermal diffusion lattices. One is non-periodic structure [Fig. 2(b)] and the other is semi-periodic structure [Fig. 2(c)]. Consider the thermal transport model with finite thermal unit cell, as illustrated in Fig. 2(a). Take the number of thermal unit cell as 4 in both the x and y direction, 8 × 8 thermal sites are arranged in a plane in thermal lattice, as illustrated in Fig. 2(b). This non-periodic thermal diffusion lattice structure is endowed with fixed boundaries by connecting the boundary sites with constant-temperature heat reservoirs via thermal channels. Additionally, a semi-periodic thermal diffusion lattice structure is proposed, as shown in Fig. 2(c). Without loss of generality, we take 8 × 8 thermal sites and then connect them head-to-tail in the x-direction, forming a periodic boundary in the x-direction and remaining a fixed boundary in the y-direction. Following Eq. (3) and Eq. (4), we can obtain the Hamiltonian of these two thermal diffusion lattice structures.

Theoretical calculations delineate the eigen spectrum of the non-periodic structure, as depicted in Fig. 2(d). When $\delta = 1$, the eigenvalues are almost uniformly distributed. When $\delta < 1$, the system is under a topological trivial state. As δ decreases, indicating an increased ratio of intra-coupling to inter-coupling diffusion coefficient, the band gradually opens, and the band gap widens. Conversely, when $\delta > 1$, the system is under a topological untrivial state. As δ increases, indicating an increased ratio of inter-coupling to intra-coupling diffusion coefficient, the band also gradually opens, with additional eigenvalues appearing in the band gaps, signifying the presence of edge states. These distinctive edge states, marked with red dots, are primarily localized at the periphery of the lattice, as evidenced by their corresponding eigenvectors. Further observation of the eigen spectrum reveals that the larger δ is, the more obvious the edge states are in the energy spectrum. At the same time, it can be observed that the occurrence position of edge states in the non-periodic structure is aligned with that in the eigen spectrum in Fig. 1(d). Although this aligned position is not rigorous, this observation underscores that the occurrence of such edge states is highly dependent on the periodicity. Besides, a higher-order topological state, known as the corner state, is observed, as marked with blue dots in Fig. 2(d). The eigenvectors corresponding to the corner states are almost distributed in the corners, exhibiting identical eigenvalues. This observation contrasts sharply with the ideal model with periodic BCs in one direction. As for our semi-periodic structure, the eigen spectrum is shown in Fig. 2(e). In this structure, as δ changes, the opening process of the band is similar to that in non-periodic structure. And there also appears edge states in bandgaps when $\delta > 1$. However, the edge states that appear within the bandgaps are corresponding to eigenvectors that are primarily distributed along two opposing edges, in contrast to the four-edge distribution observed in the non-periodic structure. What's more, there will be no appearance of corner states. These differences between the non-periodic structure and the semi-periodic structure emphasize the vital effect of periodicity on the topological states in our topological thermal transport model.

Besides theoretical calculations, numerical simulations are also performed to obtain the Hamiltonian. This approach allows us to retrieve the Hamiltonian from simulated temperature field but not only theoretical calculations, which is more in line with reality. Following Eq. (4), the Hamiltonian of our model can be retrieved from the measured temperature field in simulations as

$$H_r = i\frac{\ln T_2 - \ln T_1}{t_2 - t_1} \tag{6}$$

where t_1 is the first measurement time, t_2 is the second measurement time, T_1 and T_2 denote the temperature matrix consist of all 8 × 8 thermal sites at t_1 and t_2.

We perform numerical finite-element method (FEM) simulations with COMSOL Multiphysics. The material in simulation is aluminum ($\kappa = 200\ \mathrm{W{\cdot}m^{-1}{\cdot}K^{-1}}$, $\rho = 2700\ \mathrm{kg{\cdot}m^{-3}}$, $C_p = 880\ \mathrm{J{\cdot}kg^{-1}{\cdot}K^{-1}}$) and the size parameters are as follows: $R_0 = 10$ mm, $a_0 = 40$ mm, $h = 10$ mm, R_1 and R_2 varies from 1 to 3 mm. We set 293 K as the room temperature and 343 K as the initial temperature, and then connect boundary sites to BCs with fixed room temperature. Sequentially number all thermal sites from 1 to 64. Then apply the initial temperature to each thermal site in numbered order. Finally the resulting temperatures of all thermal sites at t_1 and t_2 are obtained, forming a 1 × 64 temperature matrix. By iterating this procedure for all thermal sites, T_1 and T_2 are compiled as two 64 × 64 temperature matrices. Finally, obtain the Hamiltonian following Eq. (6) and proceed to calculate the eigen spectrum.

Fig. 3 demonstrate the eigen spectrum achieved respectively by numerical simulations and theoretical calculations, as previously described. In order to observe the band opening and the appearance of edge states more distinctly, δ is set as 1/9 and 9 under two different states. It can be observed that when $\delta = 1/9$, the system is under topological trivial state, and the eigen spectrums of non-periodic structure [Fig. 3(a)] and semi-periodic structure [Fig. 3(c)] are analogous. All thermal sites are under bulk states whether in the non-periodic structure or the semi-periodic structure. When $\delta = 9$, the system is under topological untrivial state. The eigen spectrums of the non-periodic structure [Fig. 3(b)] and the semi-periodic structure [Fig. 3(d)] are illustrated. Notably, the edge states and corner states appear, as marked by red and blue color. Consistent with previous analysis, the non-periodic structure features both edge and corner states, whereas the semi-periodic structure features only edge states. Edge and corner states can be identified by the corresponding eigenvectors. The eigenvectors corresponding to several typical topological states are shown in Fig. 3(e-h). In bulk states [Fig. 3(e)], eigenvectors exhibit an average distribution across each position, which is similar in both structures. However, the edge states of these two structures manifest different distribution characteristics. In the non-periodic structure, the eigenvector corresponding to edge state I [Fig. 3(f)] is mainly distributed at the position of four boundaries. In the semi-periodic structure, the eigenvector corresponding to the edge state II [Fig. 3(g)] is primarily distributed along the position of two opposite boundaries. This disparity arises from the semi-periodic structure's folded configuration, which transforms the four boundaries of the non-periodic structure into two, thereby influencing the eigenvector distribution. For corner states [Fig. 3(h)] which are exclusive to the non-periodic structure, the eigenvectors are entirely distributed at four corners.

Overall, the result of numerical simulations and theoretical calculations agrees well, validating the accuracy of our model in describing thermal field of the practical heat transfer structure. Although our simulation is completely based on the real geometric size and material properties, due to the simplification of thermal channels in the theoretical calculation, there is a minor error between the numerical simulations and the theoretical calculations. It is undeniable that this research lacks experimental verification to further verify this interesting phenomenon. However, through the comparison and verification of theoretical calculations and FEM numerical simulations, the significant influence of periodicity on the topological states in our topological thermal transport model is underscored and emphasized.

To investigate the temporal evolution of temperatures at sites under different topological states, we conduct numerical simulations with the two structures [Fig. 2(b) and 2(c)]. With the same BCs mentioned above, we apply the initial temperature to the thermal sites corresponding to the corner states, edge states and bulk states respectively and observe their temperature evolution. To control the diffusion coefficient ratio δ, the radii of intra-coupling and inter-coupling thermal channels are set as $R_1 = 1$ mm and $R_2 = 3$ mm or $R_1 = 3$ mm and $R_2 = 1$ mm to keep $\delta = 1/9$ or 9. For the non-periodic structure, time evolution of normalized temperature for corner, edge, and bulk states is depicted in Fig. 4(a) and 4(b). When the system is under topological untrivial state, compare the

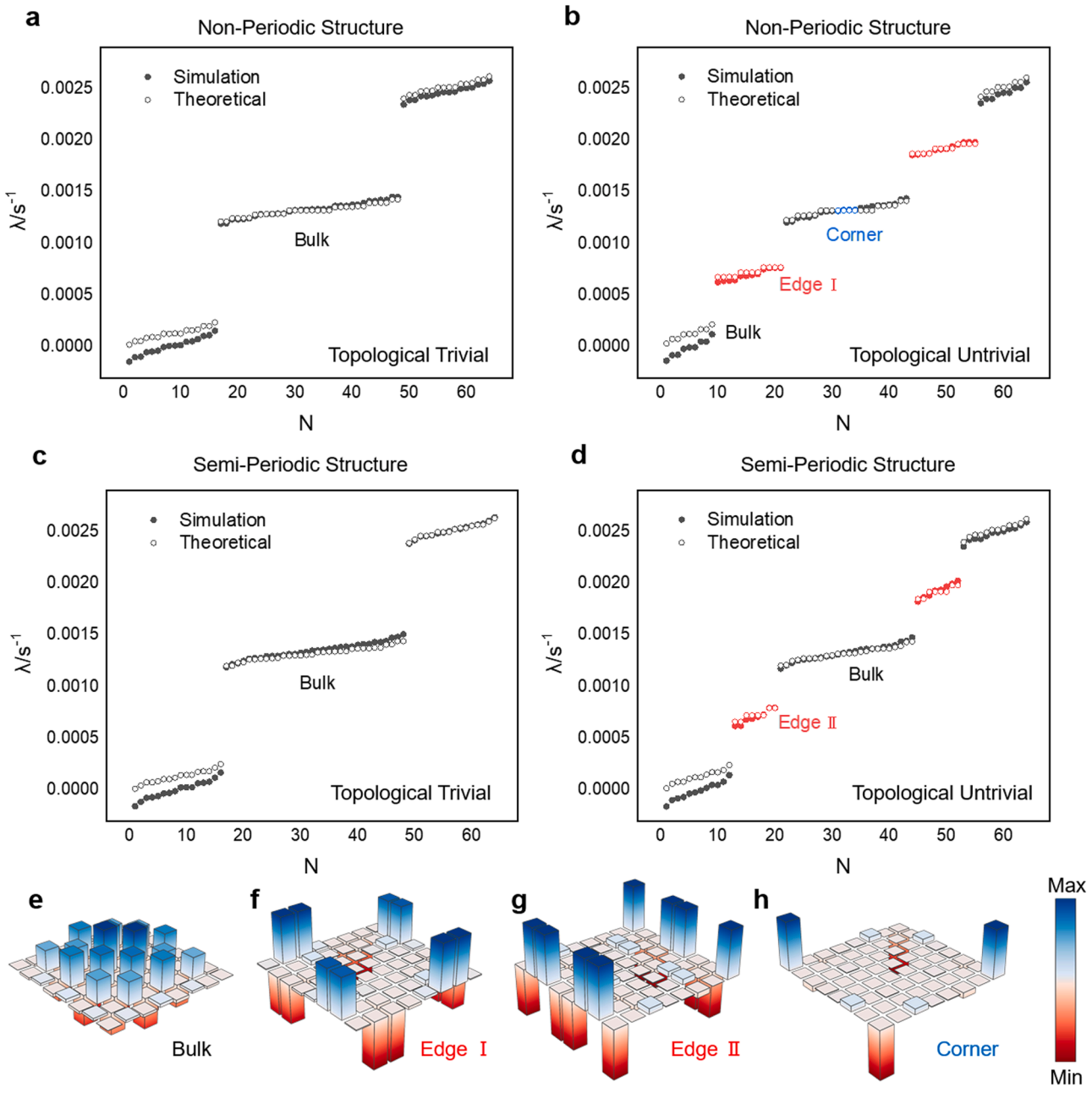

Fig. 3. (a, b) Eigen spectrum of the 8 × 8 non-periodic thermal diffusion lattice structure under topological trivial and topological untrivial state. (c, d) Eigen spectrum of the 8 × 8 semi-periodic thermal diffusion lattice structure under topological trivial and topological untrivial state. (e-h) Eigenvectors of different topological states. The color bar denotes the magnitude of each item in the eigenvectors.

decay rates of the highest temperature under these conditions. Theoretically, the eigenvalue of the system is expected to decay exponentially over time, with the decay rate being directly related to the imaginary part of the eigenvalue. A higher decay rate indicates a more rapid cooling ability. The temperature field distribution of different states is illustrated in Fig. 4(c), showing main part of the structure. After 60 s, the highest temperature of corner state has dropped to 302.28 K, while the highest temperature of edge state is 303.85 K and that of bulk state is still 306.00 K. It is evident that the highest temperature of corner state decays the fastest, followed by edge state, and that of bulk state is much slower. In contrast, when the system is under topological trivial state, although there are no corner and edge states, we apply the same initial temperature to the same position as above. In this way, we observe that the decay rate of the highest temperature is nearly uniform across different positions. After 60 s, the highest temperature of all three lattice converges to ~306 K. For Periodic Structure, there are only edge states without corner states. We observe the temperature evolution process in both topological trivial and topological untrivial states, as depicted in Fig. 4(d). The edge state under topological untrivial states exhibits the highest decay rate, corresponding to the result of theoretical calculation. Neither the bulk state under topological untrivial state nor any state under topological trivial state exhibits a stable temperature decay rate, with their temperature change trends being nearly indistinguishable. Observing the temperature field distribution after 60 s [Fig. 4(e)], the highest temperature of edge state in topological untrivial system has dropped to 309.44 K, while the highest temperatures of the other three lattices are ~312.5 K.

Through a comprehensive analysis of temperature evolution across various BCs and topological states, we find that these topological states enhance the cooling efficiency of thermal sites, with higher-order

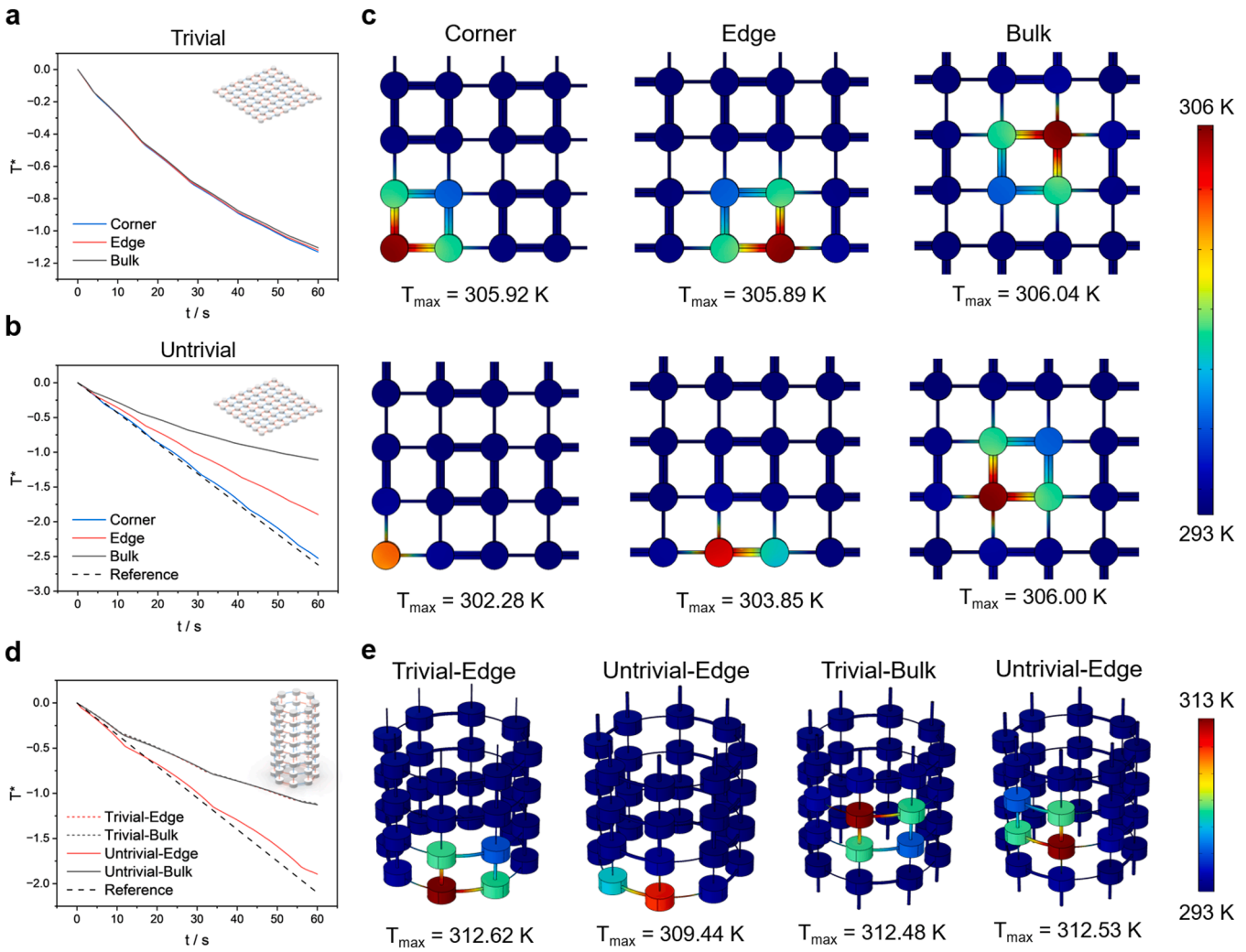

Fig. 4. Time evolution of normalized temperature of corner, edge, and bulk states under topological trivial (a) and untrivial (b) state in non-periodic structure. (c) Temperature field distribution of corner, edge, and bulk states in non-periodic structure ($t = 60$ s). (d) Time evolution of normalized temperature of edge and bulk states in semi-periodic structure (e) Temperature field distribution of edge and bulk states in semi-periodic structure ($t = 60$ s). The temperature is normalized with $T^* = \ln[(T - T_r)/(T_i - T_r)]$, where T_r is the reference temperature and T_i is temperature of thermal site at $t = 0$ s.

topological states exhibiting a more pronounced effect. It is worth mentioning that edge states and corner states appear exclusively under topological untrivial state. Therefore, the corner and edge mentioned under trivial state in the figure refers to the corresponding positions rather than being under those states. Moreover, these topological states tend to evolve with a constant decay rate, with their normalized temperatures exhibiting a linear trend. This suggests that once a thermal site is under a particular topological state, it maintains that state, forming a topological protection mechanism. Such mechanism provides a new way to realize directional and precise heat flow regulation within a complex system and holds significant potential for application of topological protected thermal metamaterials for local heating, cooling, and protection in practical thermal management.

4. Conclusion

In conclusion, we have developed a periodicity-dependent 2D topological thermal transport model and analyzed how periodicity alters topological states in both ideal and practical thermal diffusion systems. The effect of periodicity alterations in BCs on the topological state of the system is investigated, and two practical thermal diffusion models are constructed for illustration. Through both theoretical analysis and numerical simulations, the Hamiltonian of two kinds of practical thermal diffusion meta structures is obtained and the corresponding topological states are analyzed, underscoring the pivotal role of periodicity in the model. This research will motivate further exploration of topological analyses in thermal diffusion systems and pave the way for developing novel thermal metamaterials for topological thermal protection and advanced thermal management.

Data availability

Data will be made available on request.

CRediT authorship contribution statement

Zhaochen Wang: Writing – original draft, Methodology, Investigation, Conceptualization. **Tianfeng Liu:** Methodology, Investigation, Data curation. **Zhan Zhu:** Validation. **Xiaobing Luo:** Validation, Conceptualization. **Run Hu:** Writing – review & editing, Supervision, Funding acquisition, Conceptualization.

Declaration of competing interest

The authors declare that they have no known competing financial interests or personal relationships that could have appeared to influence

the work reported in this paper.

Acknowledgments

The authors acknowledge the financial support from National Key R & D Project from Ministry of Science and Technology of China (2022YFA1203100), National Natural Science Foundation of China (52422603, 52076087, 5221150005), Interdiciplinary Research Program of HUST (5003120094), and Natural Science Foundation of Hubei Province (2023AFA072).

References

[1] F. Liu, K. Wakabayashi, Novel topological phase with a zero berry curvature, Phys. Rev. Lett. 118 (2017) 076803.
[2] S. Weidemann, M. Kremer, T. Helbig, T. Hofmann, A. Stegmaier, M. Greiter, R. Thomale, A. Szameit, Topological funneling of light, Science 368 (2020) 311–314.
[3] K. von Klitzing, T. Chakraborty, P. Kim, V. Madhavan, X. Dai, J. McIver, Y. Tokura, L. Savary, D. Smirnova, A.M. Rey, C. Felser, J. Gooth, X. Qi, 40 years of the quantum Hall effect, Nat. Rev. Phys. 2 (2020) 397–401.
[4] S. Carr, S. Fang, E. Kaxiras, Electronic-structure methods for twisted moiré layers, Nat. Rev. Mater. 5 (2020) 748–763.
[5] S. Yao, Z. Wang, Edge states and topological invariants of non-Hermitian Systems, Phys. Rev. Lett. 121 (2018) 086803.
[6] E.J. Bergholtz, J.C. Budich, F.K. Kunst, Exceptional topology of non-Hermitian systems, Rev. Mod. Phys. 93 (2021) 015005.
[7] W.A. Benalcazar, B.A. Bernevig, T.L. Hughes, Quantized electric multipole insulators, Science 357 (2017) 61–66.
[8] L. Lu, K. Ding, E. Galiffi, X. Ma, T. Dong, J.B. Pendry, Revealing topology with transformation optics, Nat. Commun. 12 (2021) 6887.
[9] J.-W. Liu, F.-L. Shi, K. Shen, X.-D. Chen, K. Chen, W.-J. Chen, J.-W. Dong, Antichiral surface states in time-reversal-invariant photonic semimetals, Nat. Commun. 14 (2023) 2027.
[10] M. Li, D. Zhirihin, M. Gorlach, X. Ni, D. Filonov, A. Slobozhanyuk, A. Alù, A. B. Khanikaev, Higher-order topological states in photonic kagome crystals with long-range interactions, Nat. Photonics 14 (2020) 89–94.
[11] B. Hu, Z. Zhang, Z. Yue, D. Liao, Y. Liu, H. Zhang, Y. Cheng, X. Liu, J. Christensen, Anti-parity-time symmetry in a Su-Schrieffer-Heeger sonic lattice, Phys. Rev. Lett. 131 (2023) 066601.
[12] X.-D. Chen, W.-M. Deng, F.-L. Shi, F.-L. Zhao, M. Chen, J.-W. Dong, Direct Observation of corner states in second-order topological photonic crystal slabs, Phys. Rev. Lett. 122 (2019) 233902.
[13] B.-Y. Xie, G.-X. Su, H.-F. Wang, H. Su, X.-P. Shen, P. Zhan, M.-H. Lu, Z.-L. Wang, Y.-F. Chen, Visualization of higher-order topological insulating phases in two-dimensional dielectric photonic crystals, Phys. Rev. Lett. 122 (2019) 233903.
[14] Y. Ding, Y. Peng, Y. Zhu, X. Fan, J. Yang, B. Liang, X. Zhu, X. Wan, J. Cheng, Experimental demonstration of acoustic Chern insulators, Phys. Rev. Lett. 122 (2019) 014302.
[15] A.B. Khanikaev, R. Fleury, S.H. Mousavi, A. Alù, Topologically robust sound propagation in an angular-momentum-biased graphene-like resonator lattice, Nat. Commun. 6 (2015) 8260.
[16] L. Luo, H.-X. Wang, Z.-K. Lin, B. Jiang, Y. Wu, F. Li, J.-H. Jiang, Observation of a phononic higher-order Weyl semimetal, Nat. Mater. 20 (2021) 794–799.
[17] P. Jin, J. Liu, L. Xu, J. Wang, X. Ouyang, J.-H. Jiang, J. Huang, Tunable liquid–solid hybrid thermal metamaterials with a topology transition, Proc. Natl. Acad. Sci. 120 (2023) e2217068120.
[18] G. Xu, Y. Yang, X. Zhou, H. Chen, A. Alù, C.-W. Qiu, Diffusive topological transport in spatiotemporal thermal lattices, Nat. Phys. 18 (2022) 450–456.
[19] G. Xu, W. Li, X. Zhou, H. Li, Y. Li, S. Fan, S. Zhang, D.N. Christodoulides, C.-W. Qiu, Observation of Weyl exceptional rings in thermal diffusion, Proc. Natl. Acad. Sci. 119 (2022) e2110018119.
[20] G. Xu, X. Zhou, Y. Li, Q. Cao, W. Chen, Y. Xiao, L. Yang, C.-W. Qiu, Non-Hermitian chiral heat transport, Phys. Rev. Lett. 130 (2023) 266303.
[21] Z. Zhang, L. Xu, T. Qu, M. Lei, Z.-K. Lin, X. Ouyang, J.-H. Jiang, J. Huang, Diffusion metamaterials, Nat. Rev. Phys. 5 (2023) 218–235.
[22] F. Yang, Z. Zhang, L. Xu, Z. Liu, P. Jin, P. Zhuang, M. Lei, J. Liu, J.-H. Jiang, X. Ouyang, F. Marchesoni, J. Huang, Controlling mass and energy diffusion with metamaterials, Rev. Mod. Phys. 96 (2024) 015002.
[23] Ju Ran, G. Xu, L. Xu, M. Qi, D. Wang, P. Cao, R. Xi, Y. Shou, H. Chen, C. Qiu, Y. Li, Convective thermal metamaterials: exploring high-efficiency, directional, and wave-like heat transfer, Adv. Mater. (2023) 2209123.
[24] Y. Li, W. Li, T. Han, X. Zheng, J. Li, B. Li, S. Fan, C.-W. Qiu, Transforming heat transfer with thermal metamaterials and devices, Nat. Rev. Mater. 6 (2021) 488–507.
[25] R. Hu, Y. Liu, S. Shin, S. Huang, X. Ren, W. Shu, J. Cheng, G. Tao, W. Xu, R. Chen, X. Luo, Emerging materials and strategies for personal thermal management, Adv. Energy Mater. 10 (2020) 1903921.
[26] Z. Zhu, Z. Wang, T. Liu, B. Xie, X. Luo, W. Choi, R. Hu, Arbitrary-shape transformation multiphysics cloak by topology optimization, Int. J. Heat Mass Transf. 222 (2024) 125205.
[27] W. Sha, M. Xiao, J. Zhang, X. Ren, Z. Zhu, Y. Zhang, G. Xu, H. Li, X. Liu, X. Chen, L. Gao, C.-W. Qiu, R. Hu, Robustly printable freeform thermal metamaterials, Nat. Commun. 12 (2021) 7228.
[28] Z. Wang, Z. Zhu, T. Liu, R. Hu, Inverse design of thermal metamaterials with holey engineering strategy, J. Appl. Phys. 132 (2022) 145102.
[29] Z. Zhu, Z. Wang, T. Liu, X. Luo, C. Qiu, R. Hu, Field-coupling topology design of general transformation multiphysics metamaterials with different functions and arbitrary shapes, Cell Reports Phys. Sci. 4 (2023) 101540.
[30] R. Hu, S. Huang, M. Wang, X. Luo, J. Shiomi, C. Qiu, Encrypted thermal printing with regionalization transformation, Adv. Mater. 31 (2019) 1807849.
[31] R. Hu, W. Xi, Y. Liu, K. Tang, J. Song, X. Luo, J. Wu, C.-W. Qiu, Thermal camouflaging metamaterials, Mater. Today 45 (2021) 120–141.
[32] M. Qi, D. Wang, P. Cao, X. Zhu, C. Qiu, H. Chen, Y. Li, Geometric phase and localized heat diffusion, Adv. Mater. (2022) 2202241.
[33] G. Xu, X. Zhou, S. Yang, J. Wu, C.-W. Qiu, Observation of bulk quadrupole in topological heat transport, Nat. Commun. 14 (2023) 3252.
[34] G. Xu, Y. Li, W. Li, S. Fan, C.-W. Qiu, Configurable phase transitions in a topological thermal material, Phys. Rev. Lett. 127 (2021) 105901.
[35] Y. Li, Y.-G. Peng, L. Han, M.-A. Miri, W. Li, M. Xiao, X.-F. Zhu, J. Zhao, A. Alù, S. Fan, C.-W. Qiu, Anti–parity-time symmetry in diffusive systems, Science 364 (2019) 170–173.
[36] T. Yoshida, Y. Hatsugai, Bulk-edge correspondence of classical diffusion phenomena, Sci. Rep. 11 (2021) 888.
[37] C.-A. Li, Topological states in two-dimensional Su-Schrieffer-Heeger models, Front. Phys. 10 (2022) 861242.
[38] Z. Liu, P. Cao, L. Xu, G. Xu, Y. Li, J. Huang, Higher-order topological in-bulk corner state in pure diffusion systems, Phys. Rev. Lett. 132 (2024) 176302.
[39] N. Okuma, K. Kawabata, K. Shiozaki, M. Sato, Topological origin of non-Hermitian skin effects, Phys. Rev. Lett. 124 (2020) 086801.
[40] L.-W. Wang, Z.-K. Lin, J.-H. Jiang, Non-Hermitian topological phases and skin effects in kagome lattices, Phys. Rev. B 108 (2023) 195126.
[41] P.-C. Cao, Y. Li, Y.-G. Peng, M. Qi, W.-X. Huang, P.-Q. Li, X.-F. Zhu, Diffusive skin effect and topological heat funneling, Commun. Phys. 4 (2021) 230.
[42] H. Wu, H. Hu, X. Wang, Z. Xu, B. Zhang, Q.J. Wang, Y. Zheng, J. Zhang, T.J. Cui, Y. Luo, Higher-order topological states in thermal diffusion, Adv. Mater. 35 (2023) 2210825.
[43] H. Hu, S. Han, Y. Yang, D. Liu, H. Xue, G. Liu, Z. Cheng, Q.J. Wang, S. Zhang, B. Zhang, Y. Luo, Observation of topological edge states in thermal diffusion, Adv. Mater. 34 (2022) 2202257.